International Collaboration on Advanced Neutron Sources
Tsukuba, Japan, October 21-26, 1990

OPTICAL NEUTRON POLARIZERS

John B. Hayter
Oak Ridge National Laboratory
FEDC/MS-8218
P.O. Box 2009
Oak Ridge, TN 37831-8218, U.S.A.

OPTICAL NEUTRON POLARIZERS

John B. Hayter
Oak Ridge National Laboratory
FEDC/MS-8218
P.O. Box 2009
Oak Ridge, TN 37831-8218, U.S.A.

ABSTRACT

A neutron wave will be refracted by an appropriately varying potential. Optical neutron polarizers use spatially varying, *spin-dependent* potentials to refract neutrons of opposite spin states into different directions, so that an unpolarized beam will be split into two beams of complementary polarization by such a device. This paper will concentrate on two methods of producing spin-dependent potentials which are particularly well-suited to polarizing cold neutron beams, namely thin-film structures and field-gradient techniques. Thin-film optical devices, such as *supermirror* multilayer structures, are usually designed to deviate only one spin-state, so that they offer the possibility of making insertion (transmission) polarizers. Very good supermirrors may now be designed and fabricated, but it is not always straightforward to design mirror-based devices which are useful in real (divergent beam) applications, and some practical configurations will be discussed. Field-gradient devices, which are usually based on multipolar magnets, have tended to be too expensive for general use, but this may change with new developments in superconductivity. Dipolar and hexapolar configurations will be considered, with emphasis on the focussing characteristics of the latter.

I. INTRODUCTION

The momentum of a neutron will vary with changes in local potential, so that a neutron beam which passes through an inhomogeneous potential will experience refraction effects analogous to light waves. If the potential has a magnetic component, the interaction between the neutron and the field will depend on the orientation of the neutron moment, μ, relative to the field, and the refraction effects will thus be polarization dependent. This effect has been applied in a variety of techniques which produce spatial separation of the two spin states of the beam, allowing production of fully polarized beams [1]. In this article, I shall describe two basic classes of polarizing device which use such refractive effects to polarize (or analyze) neutron beams in the thermal to cold range; such devices are known as optical neutron polarizers. Attention here will be directed to the production of linear polarization; that is, beams with the neutron parallel (-) or anti-parallel (+) to the magnetic guide field direction.

The methods may be extended to produce circular (or precessing) polarization by using appropriate spin-turn devices, which are described in detail elsewhere [2]. A thorough review of neutron optics in general has been given by Klein and Werner [3].

II. THIN-FILM OPTICS

Total external (or mirror) reflection from a magnetic material has long been used to polarize neutrons. Bulk magnetic mirrors are difficult to saturate, however, and the associated magnetic circuits made such devices large and heavy. Use of easily saturated thin films of magnetic material, deposited on a substrate by sputtering or evaporation, removed this difficulty and allowed production of compact devices which could be considered routine spectrometer components. A neutron of wavelength λ which enters a material with number density N of scatterers with mean nuclear scattering amplitude b, and magnetic induction B, experiences a refractive index which is double-valued (corresponding to $2s+1$ states, $s=1/2$):

$$n_{\pm} = 1 - \lambda^2(Nb/2\pi \mp m_n(B-H)\mu/h^2) \tag{1}$$

where m_n is the neutron mass, H is the magnetic field strength, and h is Plank's constant; the signs correspond to the two possible polarization states of the neutron. The refractive index differs only slightly from unity (typically, $|n-1| \approx 10^{-5}$). An elementary application of Snell's law shows that there will be a wavelength-dependent critical angle for total reflection which is also spin-dependent:

$$(\theta_c/\lambda)_{\pm} = [Nb/\pi \mp 2m_n(B-H)\mu/h^2]^{1/2} \tag{2}$$

Inspection of eqn (2) shows that for a suitable choice of material, the critical angle will be null when $Nb = 2\pi m_n(B-H)\mu/h^2$, so that only one spin-state will be reflected. This is the basis for all thin-film optical polarizers. For commonly used materials, such as FeCo alloys, the critical angle is less than $1°\cdot nm^{-1}$. The essential features of the effect are shown in Fig. 1.
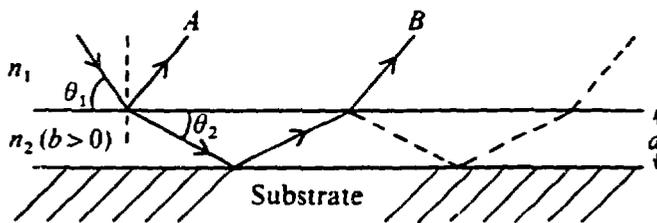
Figure 1. Reflection of neutrons from a plane parallel plate. The refractive indices in air and in the thin film are n_1 and n_2, respectively. All angles are greatly exaggerated for clarity.

The reality of the optical effects involved was shown clearly in early measurements of the reflectivity of thin-film polarizing mirrors. Constructive interference would be expected betweens the rays A and B of Fig. 1 whenever the path difference is a multiple of the wavelength. If the glancing angle θ_1 is held fixed, this leads to the expectation that interference fringes will be observed when

$$\lambda = 2(d/k) \, (\theta_1^2 - \theta_c^2)^{1/2} \qquad (\, k=1,2, \, ...) \tag{3}$$

and these fringes were indeed observed [4] (Fig. 2). The system of Fig. 1 is essentially a Lummer-Gehrke multiple-beam interferometer [5] which allows the refractive index profile of the surface to be measured, and it was recognized that this would be a valuable tool for surface studies [6]. A recent review shows that this type of measurement is now a growth industry [7].
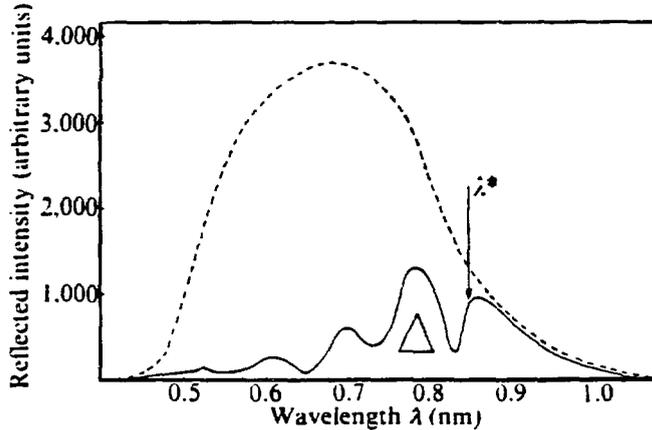

Figure 2. Neutron intensity as a function of wavelength reflected at a glancing angle $\theta=0.015$ radian from a magnetized thin film (150 nm of FeCo on glass), showing interference fringes [4]. The wavelength spectrum of the incident beam is shown dashed (not to scale) for comparison. λ^* is the critical wavelength for this material and angle. Δ represents the wavelength resolution.

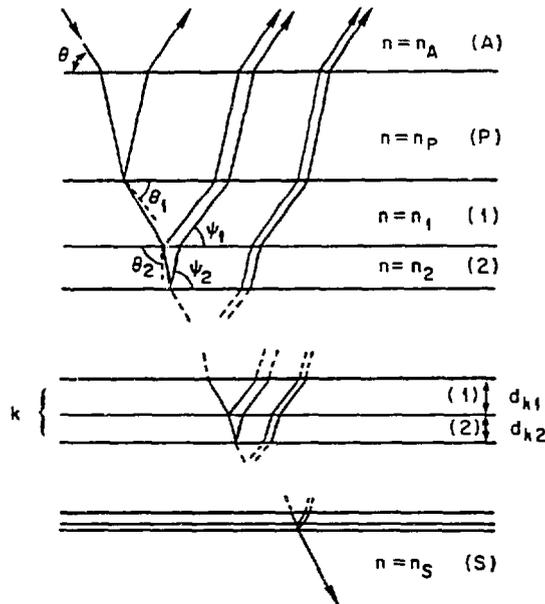Figure 3. Geometry of a general multi-bilayer structure composed of $2N$ alternating thin films of generic materials 1 and 2, having respective refractive indices n_1 and n_2, and thicknesses d_{k1} and d_{k2} in the k'th bilayer ($k=1,...,N$). The structure is assumed to lie on a substrate S and to be protected from an atmosphere A by a protective coating P. All angles have been greatly exaggerated for clarity.

The small values of θ_c have been a source of great difficulty in making use of these effects in practical spectrometers, since beam divergences often exceed the angular range of mirror reflection. Two different approaches have been taken to overcome this problem, both based on fabricating mirrors with multilayered structures. The first approach is to construct a synthetic crystal, by depositing alternating layers of magnetic and non-magnetic materials, chosen such that the matching condition derived from eqn (2) now also applies between layers for one spin state. The structure will thus act as a diffracting crystal only for the unmatched spin state, and the diffracted beam will be polarized, as well as monochromatic [8]. The second approach [9,10] is a generalization of the multilayer monochromator structure to a graded series of multi-layers, as shown in Fig. 3.

The basic physical idea behind the structure of Fig. 3, which is called a supermirror structure [9,10], is to superimpose a series of multilayer monochromator crystal structures, each of which has a slightly different d-spacing, so that the complete structure responds like a mirror, but to larger angles than would be achieved with a single layer. Apart from the obvious physical constraint that the spacing should change slowly over an extinction length, so that each "crystallite" can reflect fully, the optical problem of designing such a structure is ill-conditioned, and various designs have been proposed [9-13]; a review of the properties of such thin-film structures has been given by Majkrzak [14].

For simplicity, I shall only consider non-absorbing materials, in which case the angles ψ in Fig. 3 will coincide with the angles θ corresponding to Snell's law; in general, however, the angles θ will be complex, while the ψ are real [13]. In the absence of absorption, the angle ψ in a layer of material of type μ is related to the exterior glancing angle θ and the critical angle θ_c by

$$\psi_\mu = (\theta^2 - \theta_c^2)^{1/2} \qquad (4)$$

Optimal reflectivity from any bilayer k will occur when the bilayer acts as a $\lambda/2$ plate, with each component sublayer having $\lambda/4$ optical thickness of material μ; the equivalent physical thickness is given by

$$d_\mu = \lambda_0 / 4\psi_\mu \qquad (5)$$

Applying eqns (4) and (5) to each half of the bilayer gives the refraction-corrected expression of Bragg's law for the bilayer. It is important to note that, at low angles, Bragg peaks may shift by 20% from the positions computed without allowance for refraction, and the full expressions must be used when designing multilayer monochromator structures as well as supermirrors.

Significant improvement in the angular range of reflectivity of a mirror may be obtained by using a supermirror structure just a few bilayers thick. Figure 4(a) shows a 50% gain (FWHM) over a simple mirror, using 8 bilayers. For more ambitious mirrors, the number of layers increases rapidly, since, in the asymptotic limit of very thin layers, the thickness of the k'th layer varies as

$$d_{k\mu} \propto (\lambda_0/4\psi_\mu) \, k^{-1/4} \qquad (6)$$

and many layers must be added for a small change in angular reflectivity. Most designs have been based on continuum arguments; the best optimized is probably that of Schelten and Mika [11], an example of which is given in Fig. 4(c). More recently, a discrete thin-film multilayer (DTFM) design has been proposed [13] which provides the same response with fewer layers, and overcomes the problems of sustaining reflectivity in the vicinity of the critical edge, as shown in Fig. 4(b). Recently, experimental neutron reflectivity

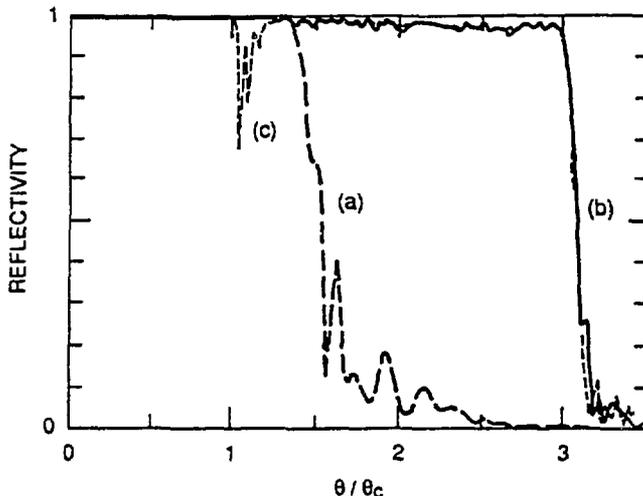data on mirrors constructed to different designs have confirmed the superiority of the DTFM structure [15].

Figure 4. Calculated neutron reflectivities for different Ni-Mn multilayer mirrors, shown as a function of glancing angle θ scaled to the critical angle for total mirror reflection, θ_c. (a) DTFM design with 16 layers total; (b) DTFM with 350 layers total; (c) continuum design of Schelten and Mika with 404 layers total. (Note the dip near the critical angle in the latter design.)

III. PRACTICAL THIN-FILM DEVICES

Successful fabrication of a polarizing supermirror structure provides only a partial answer to the problem of producing an efficient polarizing insertion device using a supermirror stack. This is because the topology of a stack is not equivalent to that of a long, flat mirror, but rather to that of a *channel*, which has quite different characteristics. A channel can only be designed for perfect reflection of an exactly parallel beam; any divergence allows some rays in the beam to be doubly reflected (Fig. 5, ray *B*), while other rays may not be reflected at all. Simulation studies of the problem (Fig. 6) show that, in general, only about 40% efficiency can be achieved for realistic systems.

One approach is to curve the channels, so that the Soller-like structure acts as a set of parallel polarizing neutron guides. If the spacing between reflecting layers is a and the radius of curvature is R, the length which corresponds to avoiding direct line-of-sight is

$$L_d = (8aR)^{1/2} \tag{7}$$

corresponding to a characteristic angle

$$\gamma^* = (2a/R)^{1/2} = L_d / 2R \tag{8}$$

Such a guide structure only transports wavelengths longer than that at which $\gamma^* = \theta_c$ which restricts the utility of such polarizing Sollers. A further disadvantage is that the exit divergence is determined by θ_c rather than the entry divergence, so that they cannot be used as insertion devices on a triple-axis spectrometer, for example, without an undesirable effect on the resolution. These devices nevertheless provided the first practical solution to
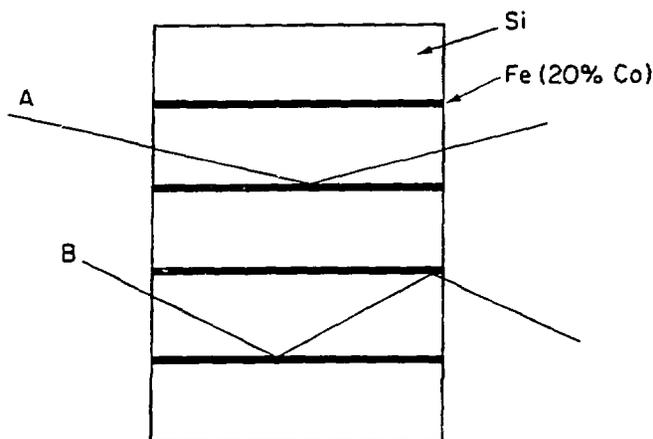
Figure 5. Schematic diagram of a mirror assembly using Si wafers. The beam enters nearly perpendicular to the Si substrate, so that glancing reflection at the air-Si interface is not possible. The mirror layers between wafers need not necessarily be the same. There is very little attenuation in the material, so that either the reflected or transmitted beams (which have opposite polarization) may be used.
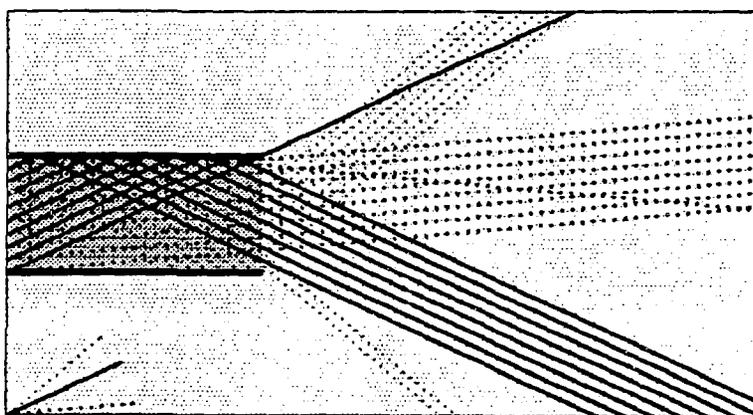

Figure 6. Transmission of a beam with 20' divergence through a supermirror stack, calculated by simulation with periodic boundary conditions at the top and bottom of the channel. The solid lines represent neutrons parallel to the mean beam direction; dotted lines are at the half-width limits of beam divergence; the relevant angles are shown at bottom left in the scaled units of the figure. If the incident angle is matched to θ_c only about 40% of the beam is reflected correctly. Increasing the incident angle allows recovery of some of the divergent neutrons, but the mean beam direction then becomes doubly reflected; efficiency remains around 40%.

the problem of producing a compact, lightweight long-wavelength polarizer [16], and were used, for example, on the first full-scale spin-echo spectrometer [17]. Many other variations on stacked practical designs have been proposed [18-20]. There is considerable incentive to improve the response of a plane, polarizing mirror stack, since such devices have many desirable properties; when used in transmission, for example, they become true insertion devices which do adversely effect spectrometer resolution. One solution is to make use

of the bandpass filter capabilities of the DTFM design [13] to place mirrors of different bandwidth strategically through a stack structure, rather than duplicating the same mirror throughout. Such structures show greatly improved handling of divergent beams (Fig. 7).
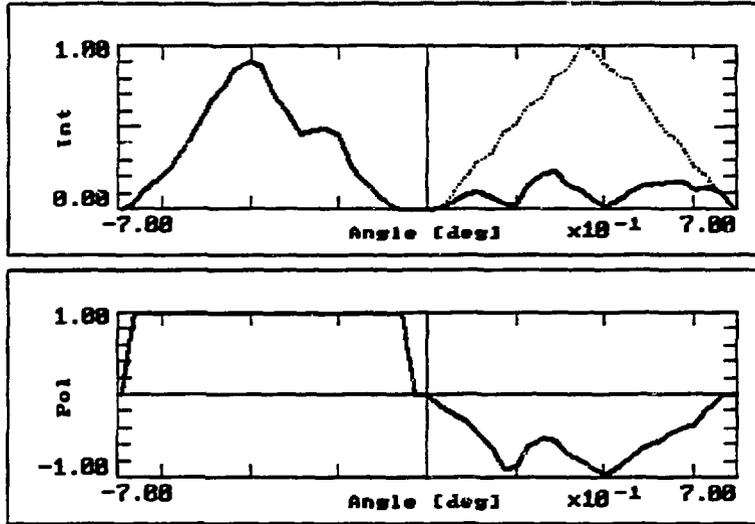

Figure 7. Intensity and polarization in a beam after transmission through a super-mirror stack made of alternating mirror types with bandpass reflection character-istics. The incident beam (dashed line) is mostly reflected (solid line) into a cleanly separated beam with about 79% efficiency and complete polarization. Results were computed by recursive simulation using 2×10^4 neutrons.

IV. FIELD-GRADIENT OPTICS

Multipolar magnetic fields provide a different means of providing a suitable optical potential gradient to separate the spin states in a beam. If the induction **B** has a gradient in the r-direction, the neutron will experience a force

$$F_r = -\partial(\boldsymbol{\mu} \cdot \mathbf{B})/\partial r \tag{9}$$

This is the well-known Stern-Gerlach effect, and it provides a useful method of measuring the absolute polarization of a linearly polarized beam, by physically separating the two polarization states into two detectors of calibrated efficiency. It is not a generally useful way of polarizing a spectrometer beam, however, since the separated beams have asymmetric divergence characteristics. The latter problem may be overcome by using a hexapolar magnet geometry [21]. For a cylindrical hexapole magnet with current distribution

$$J = J_0 \cos 3\varphi \tag{10}$$

where φ is the azimuthal angle, the radial and angular field components are

$$B_r = -B_0 \, (r/R)^2 \sin 3\varphi$$

$$B_\varphi = -B_0 \, (r/R)^2 \cos 3\varphi \tag{11}$$

where B_0 is the field at R, the inner radius of the conductor. The absolute value of the field is then independent of φ, depending only on the radius r from the central axis:

$$|B| = B_0 \, (r/R)^2 \tag{12}$$

The force on a neutron in such a field is therefore proportional to r and is directed radially inwards or outwards, depending on the neutron spin direction in the field:

$$F = \pm 2\mu B_0 \, r/R^2 \tag{13}$$

This radial force leads to equations of motion of the neutron having the form

$$\partial^2 x_i / \partial t^2 = \pm \omega^2 x_i$$
$$\omega^2 = 2\mu B_0/m_n R^2 \tag{14}$$

where $r^2 = x_1^2 + x_2^2$, and the time variable is $t=z/v$, where z is the axial direction and v is the neutron velocity. Solutions to eqns (14) are of the form $\cos \omega t$ for (-) neutrons, and $\cosh \omega t$ for (+) neutrons. The latter thus diverge away from the axis, while the former oscillate about it on a path which has the interesting property that all neutrons entering parallel to the axis focus to an axial point after exit from the hexapole, at a focal length given by

$$f = |L \cot(\omega L/v)/(\omega L/v)| \tag{15}$$

independent of their radial position at entry. The calculation for a divergent beam, which is best undertaken by simulation, gives essentially the same result for typical divergences: it is possible to focus one spin state in the beam onto a focal plane with 100% polarization. (A truly axial neutron of either spin state experiences no force, so that a small beam stop needs to be placed on the axis.)

To date, hexapoles have not seen widespread use as polarizers, because the magnets required for beams typically encountered (say, 30 mm diameter) require specifications close to the limits of commercial superconducting technology. However, with recent developments likely to bring down the cost of operating superconducting magnets, they may see a renewed role in the future.

REFERENCES

1. J. B. Hayter, in *Neutron Diffraction*, ed. H. Dachs (Springer-Verlag, Berlin, 1978) p. 41.
2. J. B. Hayter, *Z. Physik*, **B31**, 117 (1978).
3. A. G. Klein and S. A. Werner, *Rep. Prog. Phys.*, 46, 259 (1983).
4. J. B. Hayter, J. Penfold and W. G. Williams, *Nature*, 262, 569 (1976).
5. M. Born and E. Wolf, in *Principles of Optics*, chap. VII (Pergamon Press, Oxford, 1970).
6. J. B. Hayter, R. R. Highfield, B. J. Pullman, R. K. Thomas, A. I. McMullen and J. Penfold, *J. Chem. Soc., Faraday Trans. I*, 77, 1437 (1981).
7. J. Penfold and R. K. Thomas, *J. Phys: Cond. Matter* (in press).

8. A. M. Saxena and B. P. Schoenborn, *Acta Cryst.*, **A33**, 805 (1977).

9. F. Mezei and P. A. Dagleish, *Commun. Phys.*, **2**, 41 (1977).

10. A. G. Gukasov, V. A. Ruban and M. N. Bedrizova, *Sov. Tech. Phys. Lett.*, **3**, 52 (1977).

11. J. Schelten and K. Mika, *Nucl. Instrum. Methods*, **160**, 287 (1979).

12. O. Schaerpf, *A.I.P. Conf. Proc.*, **89**, 182 (1982).

13. J. B. Hayter and H. A. Mook, *J. Appl. Cryst.*, **22**, 35 (1989).

14. C. F. Majkrzak, *Physica*, **136B**, 69 (1986).

15. C. F. Majkrzak, D. A. Neumann, J. R. D. Copley and D. F. R. Mildner, *NIST Reactor: Summary of Activities, July 1989 through June 1990* (in press).

16. J. B. Hayter, J. Penfold and W. G. Williams, *J. Phys. E: Sci. Instr.*, **11**, 454 (1978).

17. P. A. Dagleish, J. B. Hayter and F. Mezei, in *Neutron Spin Echo*, ed. F. Mezei (Springer-Verlag, Heidelberg, 1980) p. 66.

18. F. Mezei, *Kerntechnik*, **44**, 735 (1984).

19. L. A. de Graaf and M. Th. Rekveldt, *Kerntechnik*, **44**, 776 (1984).

20. H. A. Mook and J. B. Hayter, *Appl. Phys. Lett.*, **53**, 648 (1988).

21. B. Hamelin, N. Xiromeritis and P. Liaud, *Nucl. Instrum. Methods*, **125**, 79 (1975).